PNC TN9410 98-017

公開資料

INJECTOR TEST(2) OF PNC HIGH POWER ELECTRON LINAC

FEBRUARY, 1998

OARAI ENGINEERING CENTER

POWER REACTOR AND NUCLEAR FUEL DEVELOPMENT CORPORATION

Ⓐ

公　開　資　料
PNC TN9410 98-017
1 9 9 8 年 2 月

動燃大電流電子リニアックの入射部試験(2)

王 元林*
(谷　賢**)

要旨

"動燃大電流電子リニアックの入射部試験(1)"の報告書ではビーム電流100mA、パルス幅20μs、繰り返し1Hzおよびビーム電流 50mA、パルス幅1ms、0.5Hz、でエネルギー3.0MeVのビーム加速について報告したが、このビーム試験は、チョッパーとプリバンチャーシステムを使わない条件で実施した。入射部試験(2)では、チョッパーとプリバンチャーシステムを使用した試験を実施し、ビーム電流100mA、パルス幅3ms、繰り返し0.1Hz、エネルギー3.0MeVで非常に整ったスペクトラムの電子ビーム加速に成功した結果について報告する。

大洗工学センター 基盤技術開発センター 先進技術開発室

* 客員研究員 (南京大学 準教授)

**実施責任者

INJECTOR TEST (2)
OF
PNC HIGH POWER ELECTRON LINAC

Y.L.Wang*

Abstract

"Injector Test (1) of PNC High Power Electron Linac" was mentioned in last year report . 100mA beam with pulse length 20μs repetition rate 1Hz and 50mA beam with pulse 1ms 0.5 Hz had been accelerated to 3.0MeV successfully. The chopper and prebuncher system had not been used in that test. Now this report put emphases on the chopper and prebuncher systems tests. A good energy spectrum had been achieved using the chopper and prebuncher systems. And 100mA beam current with pulse length 3ms and repetition rate 0.1Hz was accelerated to 3.0 MeV.

---

* Frontier Technology Development Section

Oarai Engineering Center

Visiting Researcher from Nanjing University, CHINA

Contents

List of Figures

1, Introduction

The injector of PNC high power electron linac [1] consists of a gun, chopper cavity, chopper slit, prebuncher, buncher and No.1 accelerator section. The test system includes an energy analyser and beam dump. Fig.1 shows the injector test RF system of PNC high power linac. A half power from a 1MW klystron goes to the high power dummy load and another half power energizes No.1 accelerator section and buncher by 3dB directional coupler. In the buncher branch, a small part of power will energize the prebunching cavity and chopper cavity. Each branch has a phase shifter and attenuator. Fig.2 shows components on beam line in the injector test system of PNC high power linac.

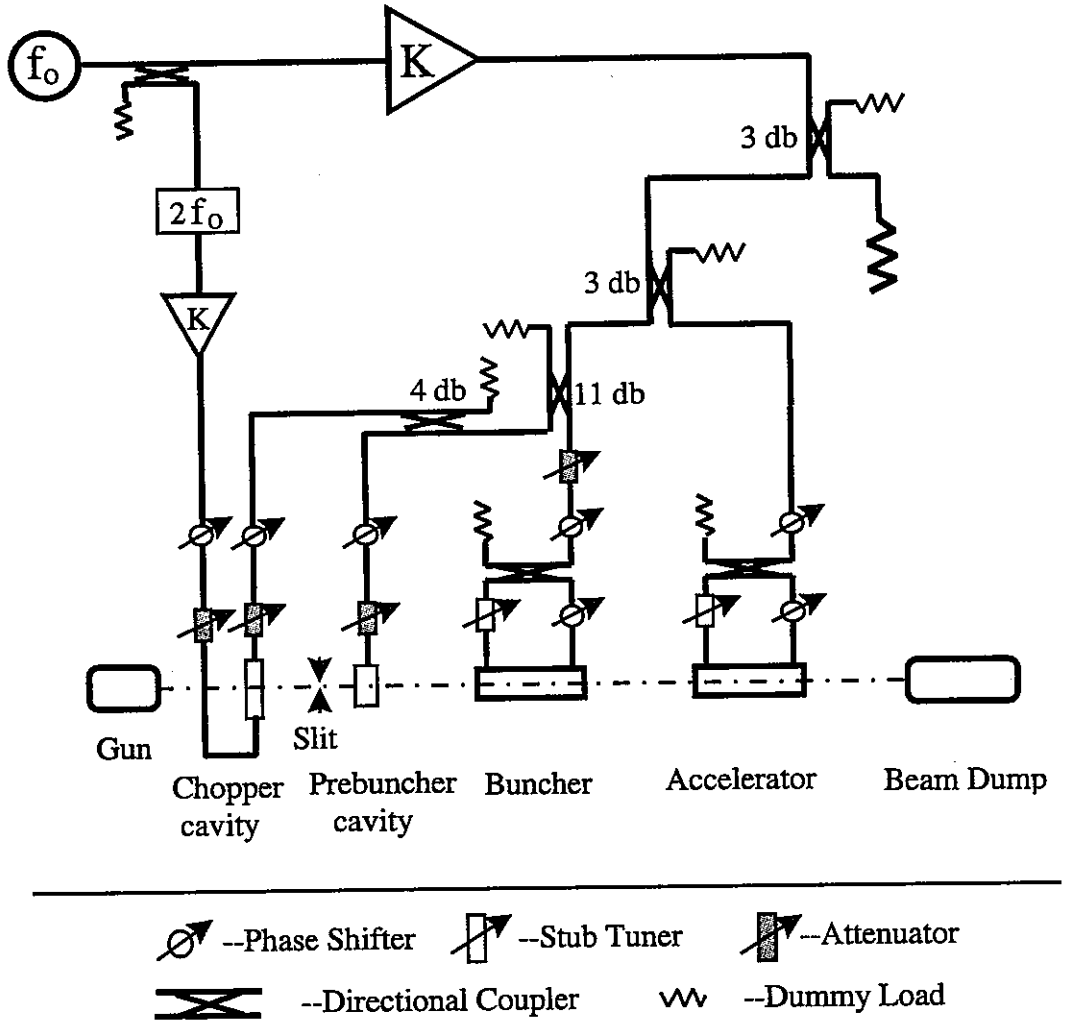

Fig.1 Injector test RF system of PNC high power linac.

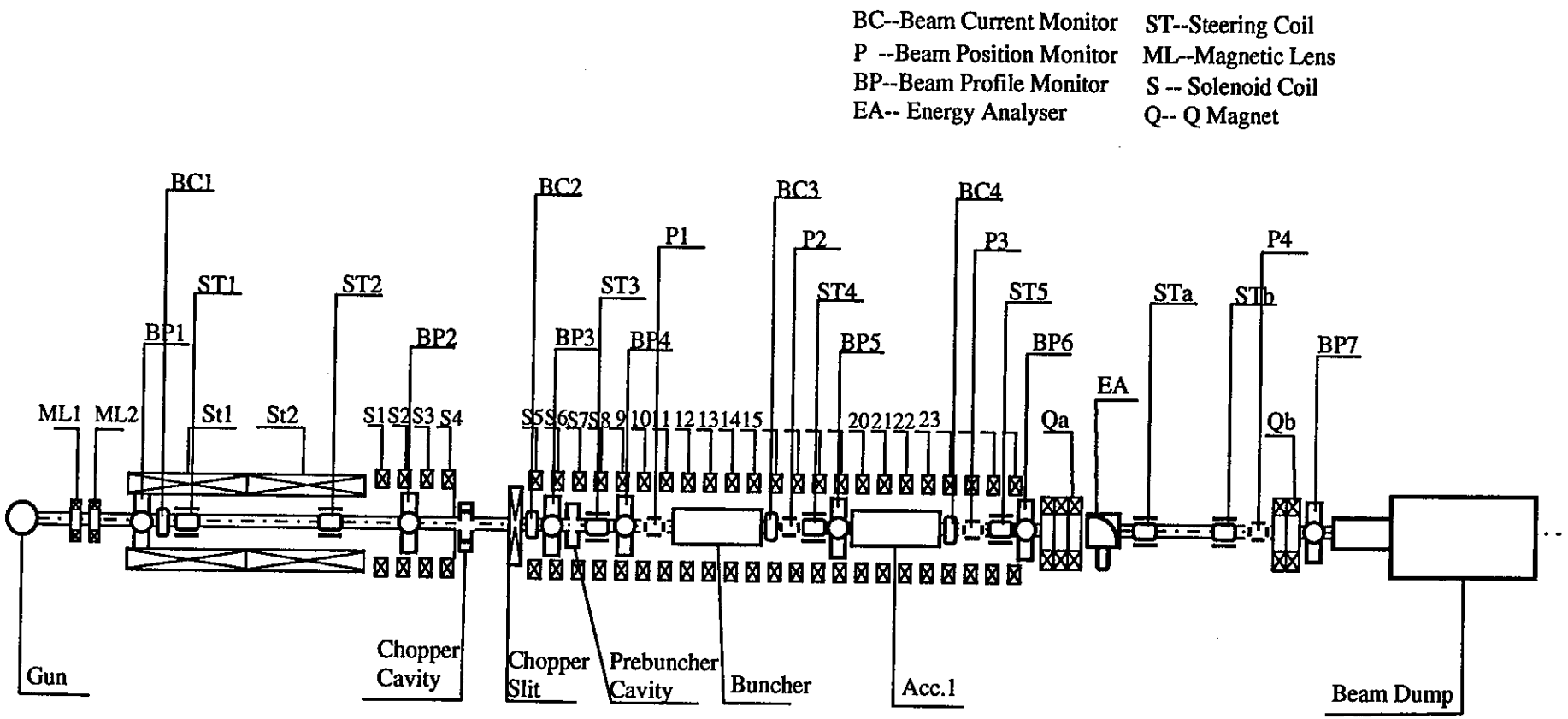

Fig.2, Components on Beam Line in Injector Test System of PNC High Power Linac

To get high duty, high beam current, small energy spread and low beam emittance, a new type chopper system and a prebuncher was adopted in the injector of PNC linac. The phase relationship of the beam bunch and RF field in the injector is shown in Fig.3. The middle plot in Fig.3 shows a phase and z axis plane; the lower plot shows an x axis and z axis plane. It is easy to understand the actions of chopping and bunching for a beam.

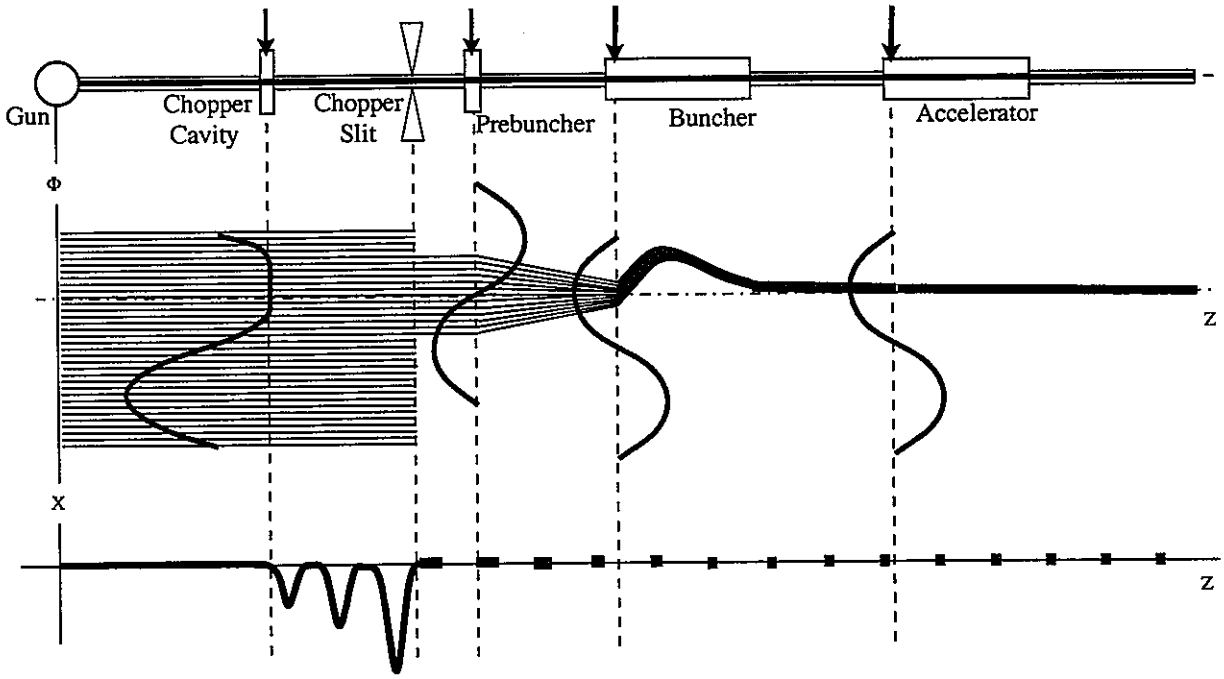

Fig. 3, The phase relationship of the beam and RF field in the injector

In a macro-pulse beam current from an electron gun is 300mA. During one microwave period, the beam in 120° phase interval can pass through the chopper system. In the macro-pulse, only 100mA beam passes through the chopper, other 200mA beam stops on the chopper slit. Then 120° chopped beam is bunched by prebuncher, after 1 meter drift it can be bunched to 25°. After that, the beam will be further bunched and accelerated by the buncher and No.1 accelerator.

2, Chopper System Test

The new type chopper cavity including a fundamental and second harmonics was developed for low emittance accelerators[2,3,4]. The low power test of the chopper system had been done [5]. For the high power and beam on line test, at first, we used fundamental frequency (f_0=1249.135MHz) power to aging the chopper cavity. During the aging, adjusting stub tuners let the cavity resonate at fundamental frequency f_0. Then we used harmonic frequency $2f_0$ power to aging

and make the cavity resonate at $2f_0$. There are two kinds of stub tuner: one called fine tuner; another side tuner. According to low power test data, we knew the frequency changing ratios of each tuner. It was easy to make the chopper cavity resonate at f_0 in TM_{210} mode and resonate at $2f_0$ in TM_{410} mode simultaneously, using following formulae to get tuning values:

$$\Delta hs_{fine} = \frac{\frac{\partial f_{210}}{\partial hs_{side}} \times \Delta f_{410} - \frac{\partial f_{410}}{\partial hs_{side}} \times \Delta f_{210}}{\frac{\partial f_{210}}{\partial hs_{side}} \times \frac{\partial f_{410}}{\partial hs_{fine}} - \frac{\partial f_{410}}{\partial hs_{side}} \times \frac{\partial f_{210}}{\partial hs_{fine}}}$$

$$\Delta hs_{side} = \frac{\Delta f_{210} - \frac{\partial f_{210}}{\partial hs_{fine}} \times \Delta hs_{fine}}{\frac{\partial f_{210}}{\partial hs_{side}}}$$

After that let the chopper slit full open (40mm). A 10mA beam from the gun with a low duty factor(10μs,1Hz) passed through the chopper cavity and slit. There is a beam profile monitor after the chopper slit. When the chopper cavity without any RF power, the beam profile was a circle shown in Fig.4 (a). While a RF power with frequency f_0 was added in chopper cavity, the beam deflected in x direction both sides, the beam profile spread in x direction which shown in Fig.4 (b). The larger RF power, the longer beam profile in x direction. When the f_0 power was 400w, the beam spread about 40mm in x direction. When DC magnetic bias was added, the beam profile moved to one side in x direction, it is shown in fig.4 (c). After that it was a key point of this new idea, a RF power with frequency $2f_0$ was added in the chopper cavity too, adjusting its amplitude and the phase made the field in the cavity had a flat part, the waveforms are shown in Fig.5. Fig.5, (a) shows a waveform with frequency f_0 and power 397.8W, Fig.5, (b) shows a waveform with frequency $2f_0$ and power 46.6W, Fig.5, (c) shows the waveform of f_0 and $2f_0$ fields' superposition, there is a 120° flat part, by means of Communication Signal Analyser CSA803. Fig.6 shows the chopper cavity connected with the Communication Signal Analyser CSA803. In that case, the beam profile is shown in Fig.4 (d). The difference between the Fig.4 (c) and (d) is that in the left end of the beam profile in Fig.4 (d) is brighter and shorter than the left end in Fig.4 (c). Because the left end in Fig.4 (d) is the flat part of the beam corresponding to the flat part of the waveform, it includes more electrons. Then we closed the chopper slit to the width equal to the beam diameter(8mm). Let the beam flat part passed through the slit. The beam profile is shown in Fig.(e). One-third beam current was got after chopper slit. The new type chopper system had already been adjusted successfully. After that we could increase the beam current and duty factor. Next, we would adjust the prebuncher.

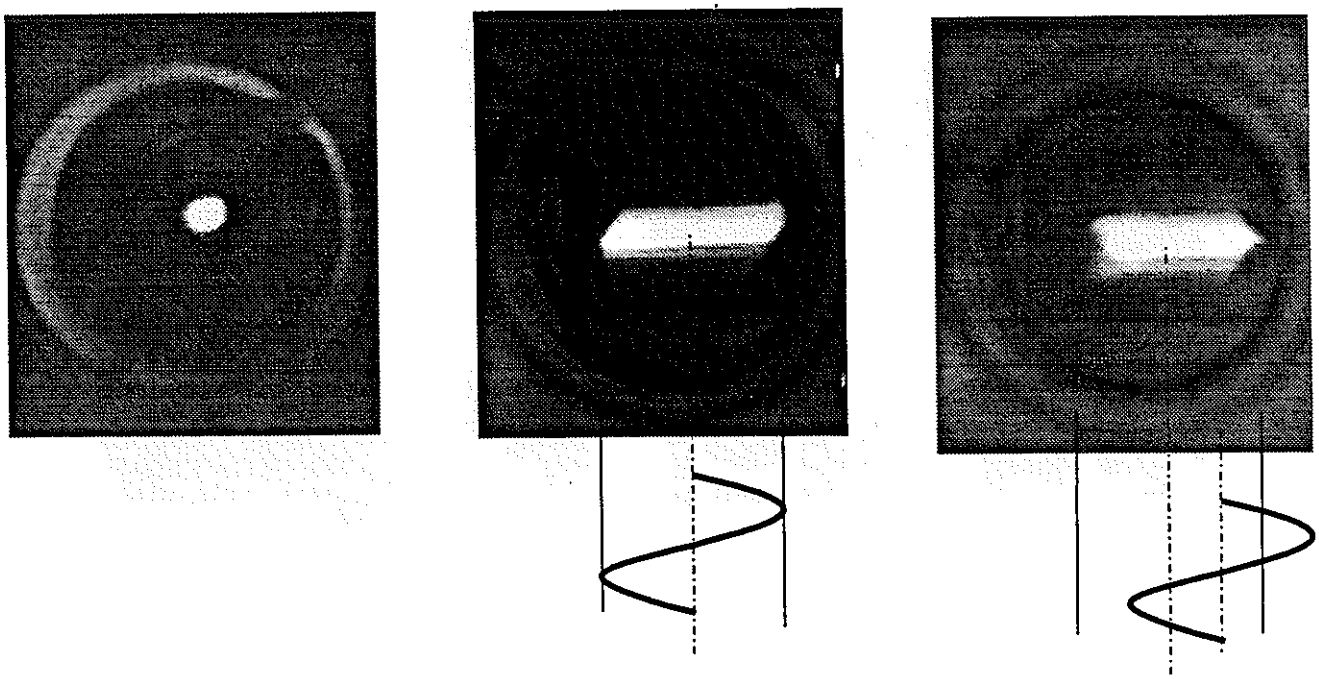

(a), chopper cavity without field

(b), chopper cavity with f_0 field

(c), with f_0 field and DC bias

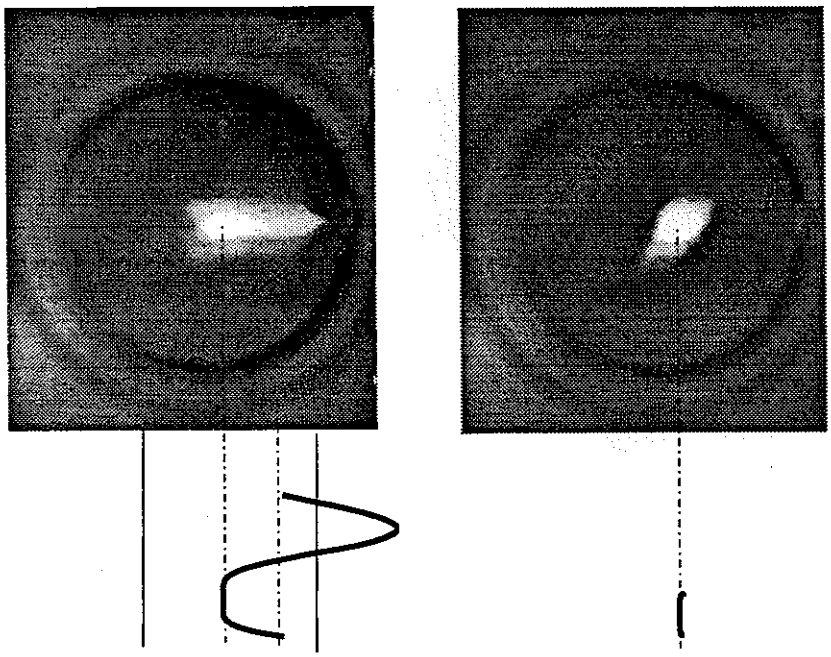

(d), with f_0 and $2f_0$ fields and DC bias

(e), with f_0 and $2f_0$ fields and DC bias slit width 8mm

Fig.4 Beam profiles after chopper slit during adjustment

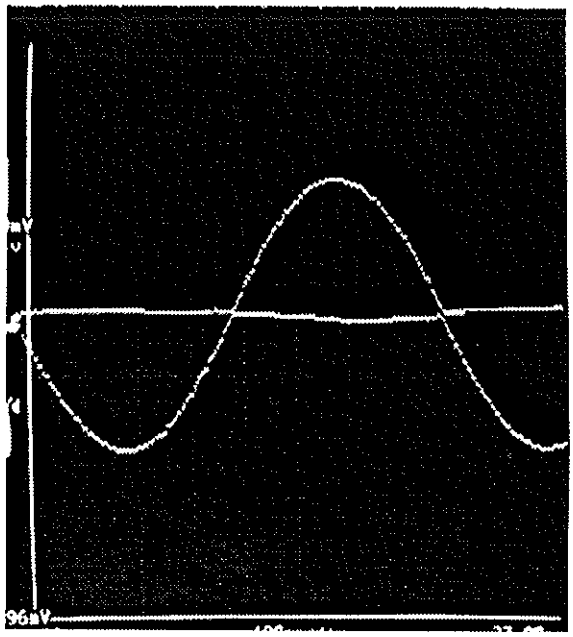

(a), f_0 waveform

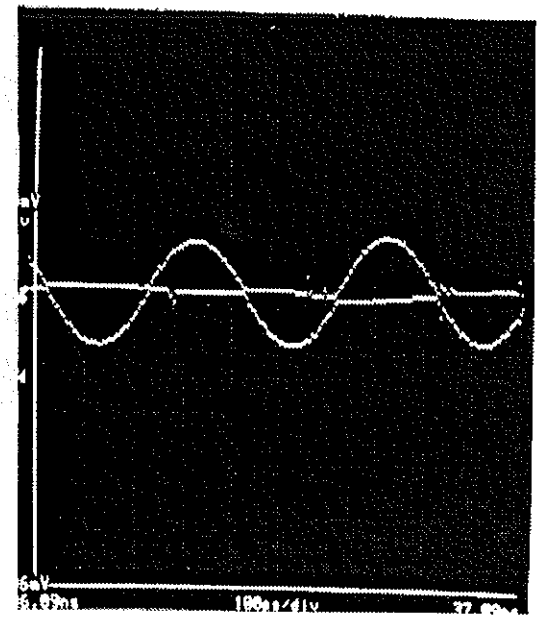

(b), $2f_0$ waveform

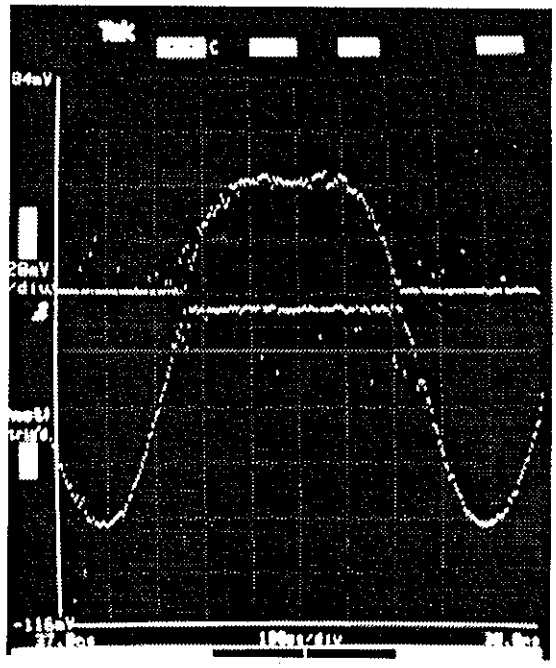

(c), $f_0 + 2f_0$ waveform

Fig.5 Waveforms in the chopper cavity
by means of Communication Signal Analyser CSA803

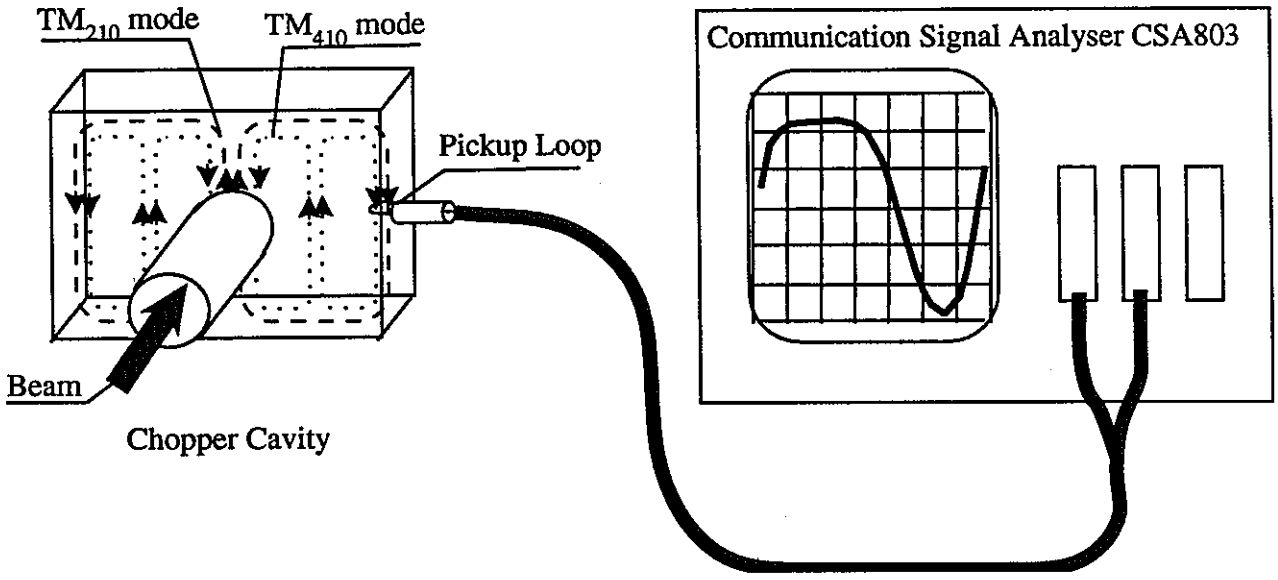

Fig. 6 Chopper cavity connected with CSA803

3, Prebuncher

3-1, Design Consideration

The beam current from the gun is 300mA. The voltage of the gun is 200kV. After RF chopper cavity, during one RF period, a beam with 120° bunch length passes through the chopper slit. The beam current is 100mA. It is preferable to choose a low voltage of a prebuncher cavity gap to decrease the energy spread. According to dynamic calculations by PARMELA, including space charge factor, the results are that the voltage of cavity gap Vg=15kV, the distance of drift between the prebuncher cavity and buncher L=1.0m, 120° bunch length of the beam can be bunched to 25°. Fig.7 shows the result of dynamic calculation.

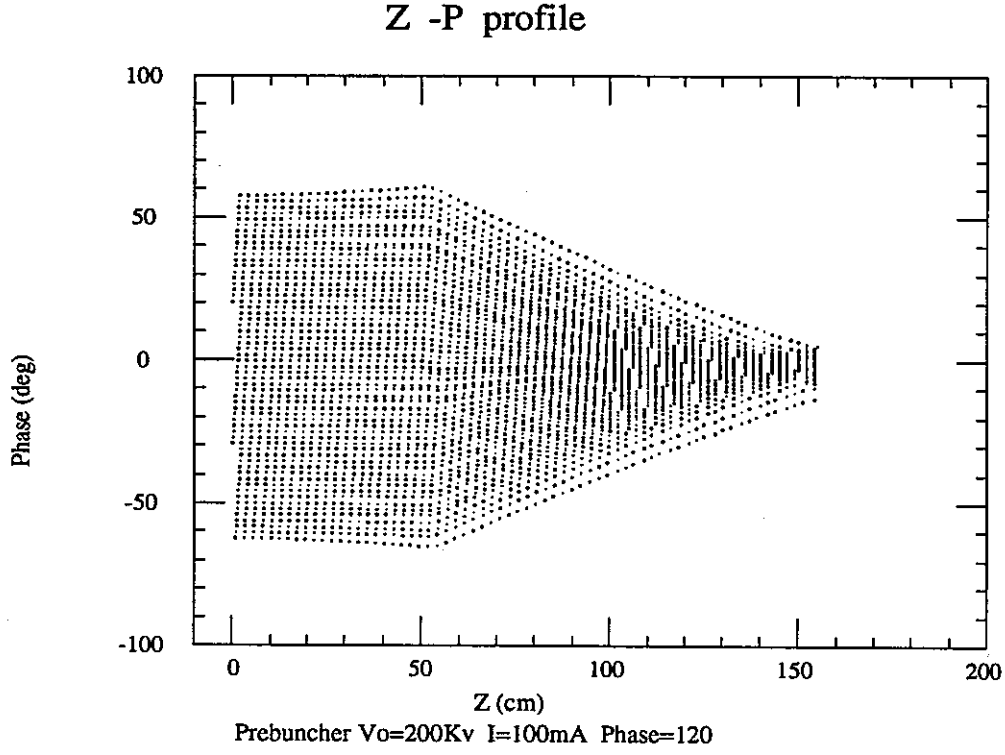

Fig.7, Result of dynamic calculation for Prebuncher Cavity by PARMELA

If a TM_{010} mode prebuncher cavity is constructed entirely from OFC(Oxygen Free Copper), it has an unloading Q of 11550 and shunt impedance of 1.1MΩ/cavity (including transit time effects).

In consideration of phase stability, high Q value will result in a sensitive phase

dependence on frequency and temperature, and the increased wall power losses caused by low Q value. A compromise method is that the cavity is constructed from a combination of OFC and SUS(Stainless Steel). Two end plats including noses are made of OFC and the surrounding body is made of SUS. The unloading Q value is 4336 and shunt impedance is 0.413MΩ/cavity.

The real prebuncher cavity is shown in Fig. 8. There are two stub tuners for cavity detuning and one offset cut for the field symmetry.

In the PNC high power linac, the prebuncher cavity is located at after chopper slit. The bunched beam induced fields will be considerable to compare with RF field.

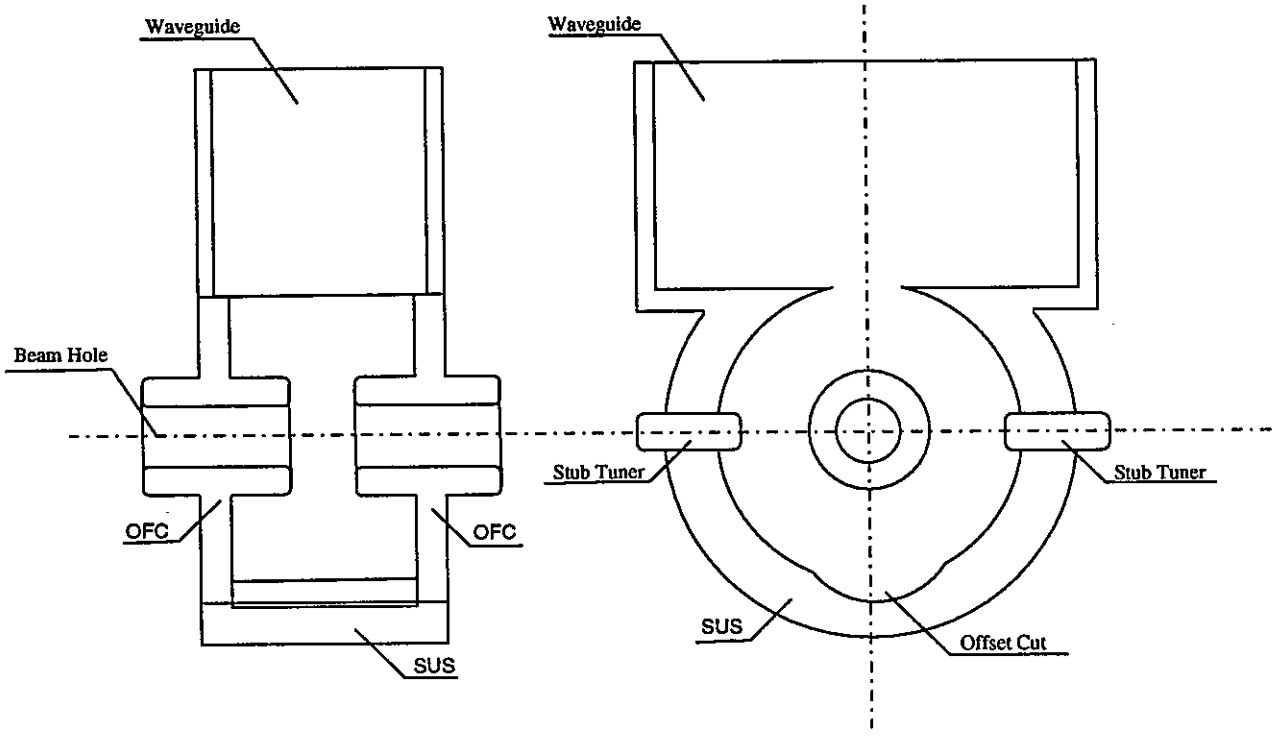

Fig.8, Prebuncher Cavity

3-2, Cavity with Beam Loading and Cavity Detuning

Fig.9 shows the equivalent circuit of the prebuncher cavity with beam loading. I_g is exciting current from a generator, I_b is beam current for induced field i.e. Fourier fundamental component of the bunched beam, I_o is Fourier DC component of the bunched beam. For short bunches, $I_b \approx 2I_o$. But for PNC the bunch length after chopper is about 120°, so $I_b = 1.65\ I_o$. β is coupling coefficient, G, L and C are conductance, inductance and capacitance of the cavity respectively. V_c is voltage of the cavity gap with beam loading.

$G = 2/R_o$
$V_g = I_g/G/(1+\beta)$
$V_b = I_b/G/(1+\beta)$

Where R_o is shunt impedance of the cavity, V_g voltage of the cavity gap only by generator current excited, V_b beam induced field voltage.

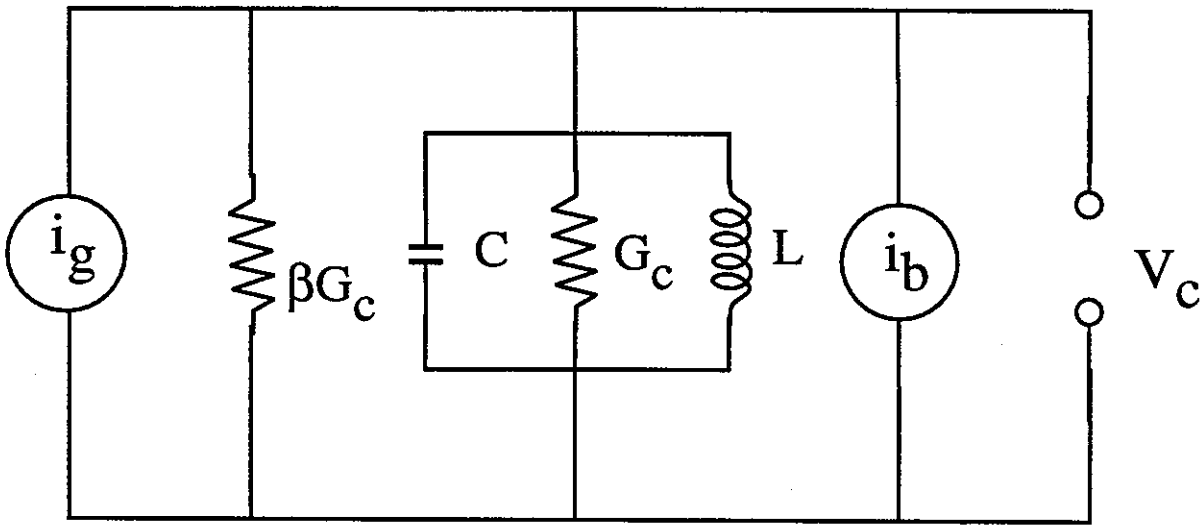

Fig.9 Equivalent circuit of the prebuncher cavity with beam loading

Let's define that the phase between beam bunch and the crest of RF electric field in the cavity is θ. The beam induced field is always located at an opposite phase with beam bunch.

If one chooses the phase of a beam bunch center for a reference phase, in this reference frame, the phase relationships are shown in Fig.10.

The vectors

$V_g = |V_g| e^{j\theta}$
$V_b = |V_b| e^{j\pi}$

and

$V_c = V_g + V_b = |V_c| e^{j\varphi}$

The amplitude V_g and angle θ is under external control by means of an attenuator and phase shifter in the waveguide system before the prebuncher cavity respectively. In the prebuncher cavity, the angle θ is chosen -90° (θ = -90°, beam bunched and θ = 90°, beam debunched). When the bunching beam passes through the prebuncher cavity, the beam induced field will be excited, the total field in the cavity V_c is superposition of vector V_g and V_b.

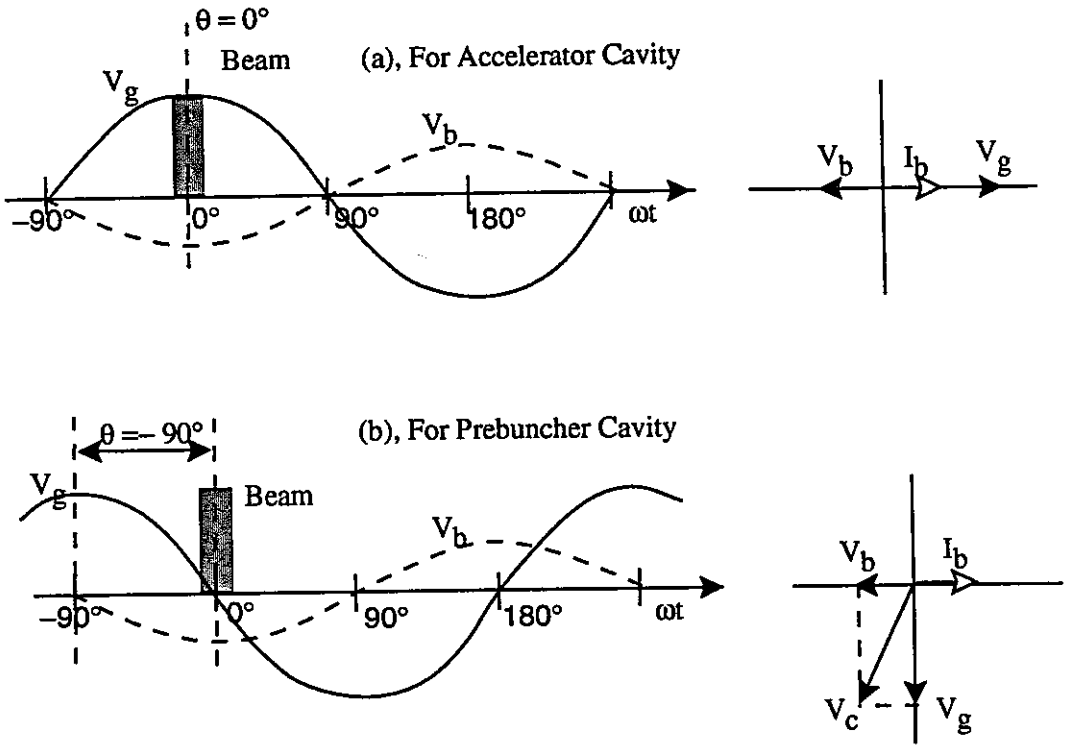

Fig.10, Phase relationships between the beam bunch and field

Detuning the cavity frequency can adjust their values to keep the total cavity voltage and angle the same as the values without beam loading.

Let's define detuning angle ψ,

$$\tan\psi = \frac{-2Q_0}{1+\beta}\frac{\omega-\omega_0}{\omega_0}$$

where ω is beam bunch angle frequency, ω_0 is the cavity resonant angle frequency. After cavity frequency detuning $\Delta\omega$, the amplitude of both V_g and V_b decrease as $\cos\psi$, and the phase of both rotate through angle ψ.

$$V_g' = |V_g \cos\psi| e^{j(\theta+\psi)}$$
$$V_b' = |V_b \cos\psi| e^{j(\pi+\psi)}$$

and

$$V_c' = V_g' + V_b' = |V_c'| e^{j\varphi'}.$$

choosing a suitable angle ψ, can make vectors $V_c' = V_g$.

Fig.11 shows the superpositions of generator and beam induced voltages, and cavity detuning actions. For generator condition, there are three cases: $\theta > -90°$, θ

= -90° and θ < -90°. For detuning, there are three cases: under, optimal and over detuning. Only in θ = -90° case, can get $V_c' = V_g$.

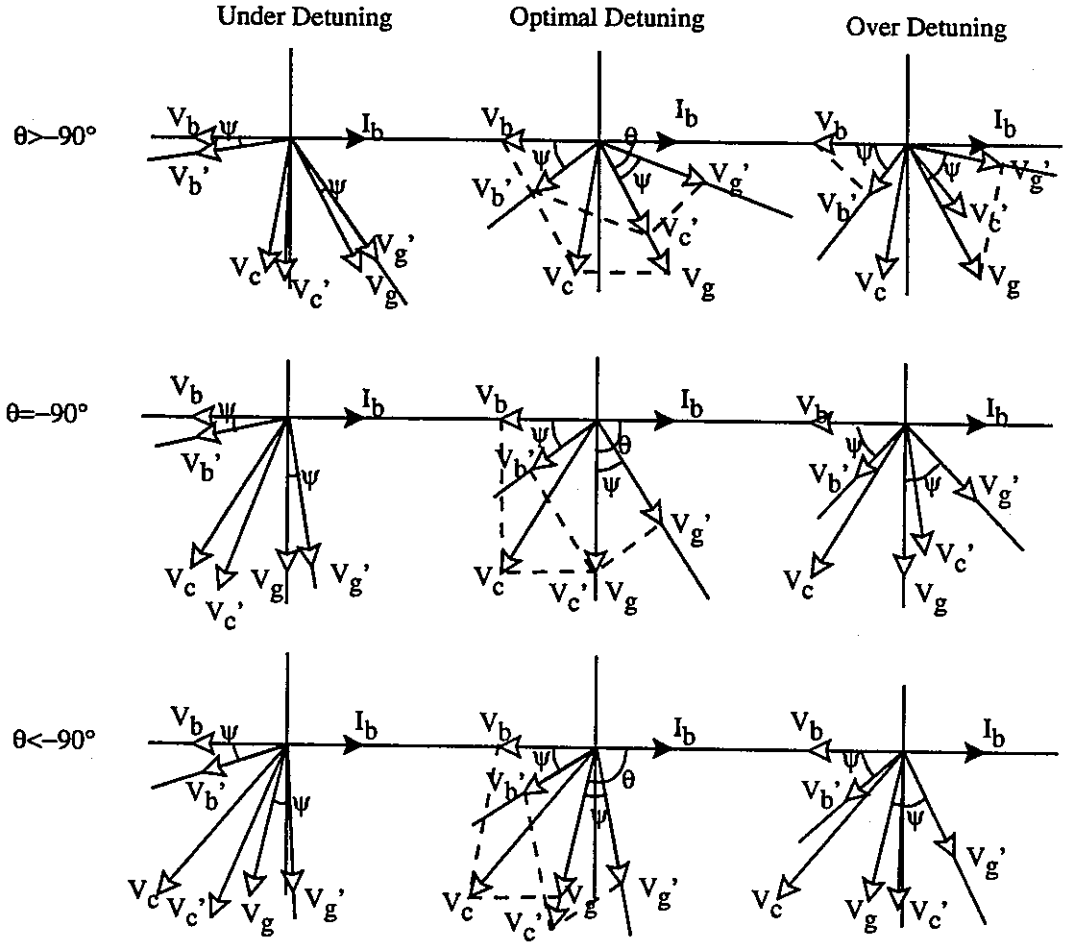

Fig.11 Superpositions of fields, and cavity detuning actions

For design we choose that θ = -90°, β = 1.0, Q = 4336, R_0 = 0.413MΩ/cavity, V_g = 15 Kv and I_b = 165mA, then we can get following data: input power for prebuncher cavity P_g = 544W, cavity detuning angle ψ = 48.6° and detuning frequency Δf = 0.32MHz.

3-3, Prebuncher Cavity Test

After the chopper system test, we tested the prebuncher cavity. The beam from the chopper slit is already chopped, the bunch length of the beam is 120°.

At first, without beam case, we adjusted the attenuator of the prebuncher branch, to make the prebuncher power 250W, then adjusted stub tuners to make the cavity resonance at 1249.135MHz and recorded the positions of stub tuners. The beam

current from the gun was 3mA, after the chopper slit was 1mA. During adjusting the phase shifter of the prebuncher branch, we found two positions of the phase shifter which were no beam loading on the RF waveform of the prebuncher cavity. The phase between the beam induced field and RF fed field at these points were 90° and 270° respectively. One was a bunching phase; another a debunching phase.

Because the adjustment of the buncher monitor had not been finished, we can not directly measure their bunch lengths to judge. Only a way was that let the beams pass through the buncher and No.1 accelerator section, then measured their energy spectra respectively. The phase in which the energy spectrum was narrower was the bunching phase.

After judging, we fixed the phase shifter at the bunching phase, recorded the amplitude and phase values for the references that shown in Fig.12 (a), then increased the beam current until 100mA, we could see changing of the beam induced field and total field. The values of the amplitude and phase are shown in Fig.12 (b) . After that, the prebuncher cavity was detuned by adjusting the stub tuners to make the values of the amplitude and phase return to the references like Fig.12 (c) shown. The superpositions of the vectors and detuning angle are shown in Fig.12 too.

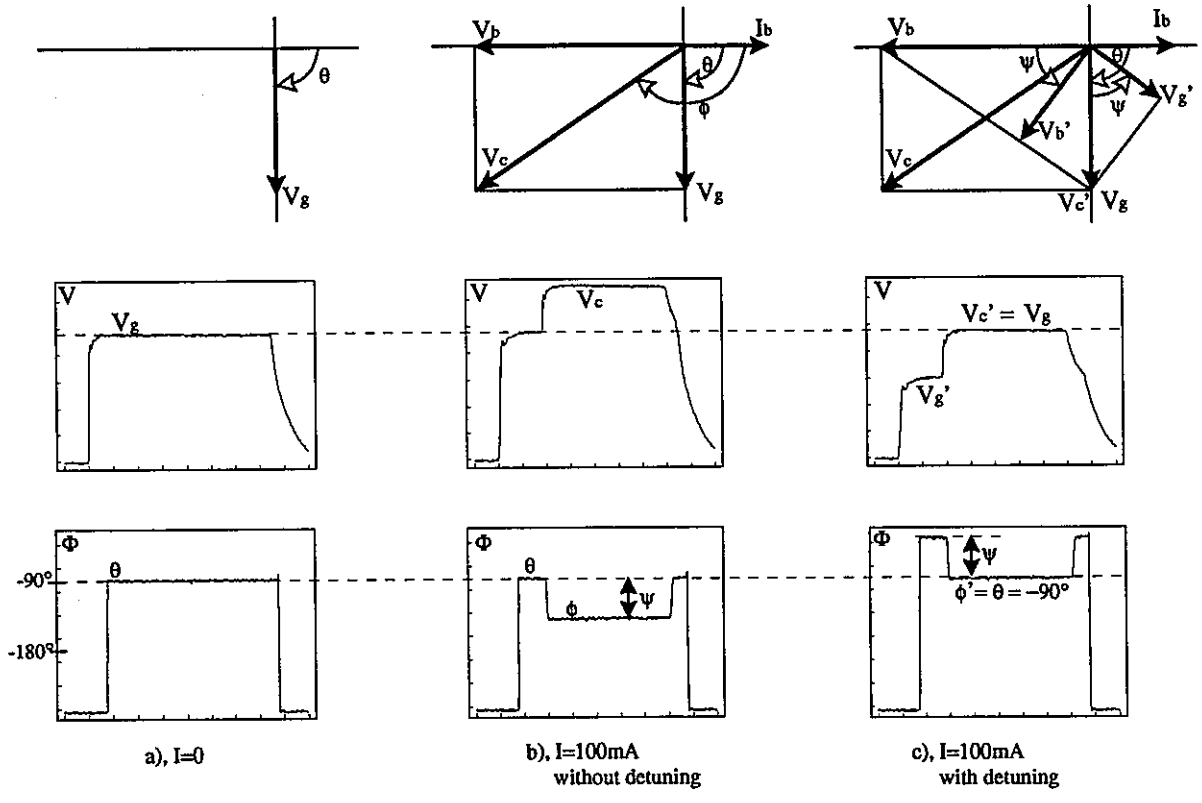

Fig. 12, Beam Loading and Cavity Detuning in Prebuncher Cavity

The adjustment of the prebuncher was finished. The power into the cavity was P_g=200W, detuning angle ψ=55° and detuning frequency Δf = 0.4MHz. Because the input power of the prebuncher cavity was lower then design, so the detuning values were a little bit larger than the design.

4, Buncher and Accelerator

After the chopper system, the 100mA chopped beam was about 120°. Then the beam was bunched by prebuncher systems. We did not know the bunch length after the prebuncher in that time. Then let this bunched beam pass through the buncher and No.1 accelerator sections. We adjusted the phase shifters of the buncher and No.1 accelerator to measure its energy spectra.. At first we needed match and tune TWRR (Traveling Wave Resonant Ring), because our buncher and accelerator sections were equiped with TWRR shown in Fig.1.

4-1, Traveling Wave Resonant Ring (TWRR) Matching and Tuning

The TWRR had already been adjusted under low power test and high power test. The positions of stub tuners were no difference between the low power and high power tests including beam loading under the beam pulse length less than 1ms. But when the beam pulse length larger than 1ms, the reflections became very large (Γ>0.2) and made the interlock system shut down the klystron power supply.

We needed to adjust the stub tuners in the TWRR to make the beam reflections small, and adjust the phase shifter in the TWRR to make the ring resonance. When the reflection with the beam was small, the reflection without the beam became large. So it would take a compromise.

Fig. 13 shows the characteristics of RF in the TWRR without and with beam loading for the short and long pulses.

The up figure shows that RF pulse length is 150μs and beam pulse 100μs. Channel 1 shows the power into the resonant ring is 188kw; Channel 2 shows the forward power in the resonant ring is 1956kw , during the 100mA beam loading, the power is 1140kw; Channel 3 shows the backward (reflection) power without beam loading in the resonant ring is 0.12kw, the reflection power with beam loading is 0.455kw; Channel 4 shows the power into the dummy load is 49.6kw and during the beam loading is 4kw.

The lower figure shows that RF pulse length is 4ms and beam pulse 3ms. Channel 1 shows the power into the resonant ring is 205kw; Channel 2 shows the forward power in the resonant ring is 1865kw , during the 100mA beam loading, the power is 933kw; Channel 3 shows the backward (reflection) power without beam loading in the resonant ring is 1.86kw, the reflection power with beam loading is 0.6kw; Channel 4 shows the power going to the dummy load is 45.7kw and during the beam loading is 0.4kw.

From these figures we can see that:

1), The multiplication factor of TWRR without beam loading M=3.22 and with beam loading M_b=2.46 for a short pulse, the multiplication factor of TWRR without beam loading M=3.01 and with beam loading M_b=2.13 for a long pulse.

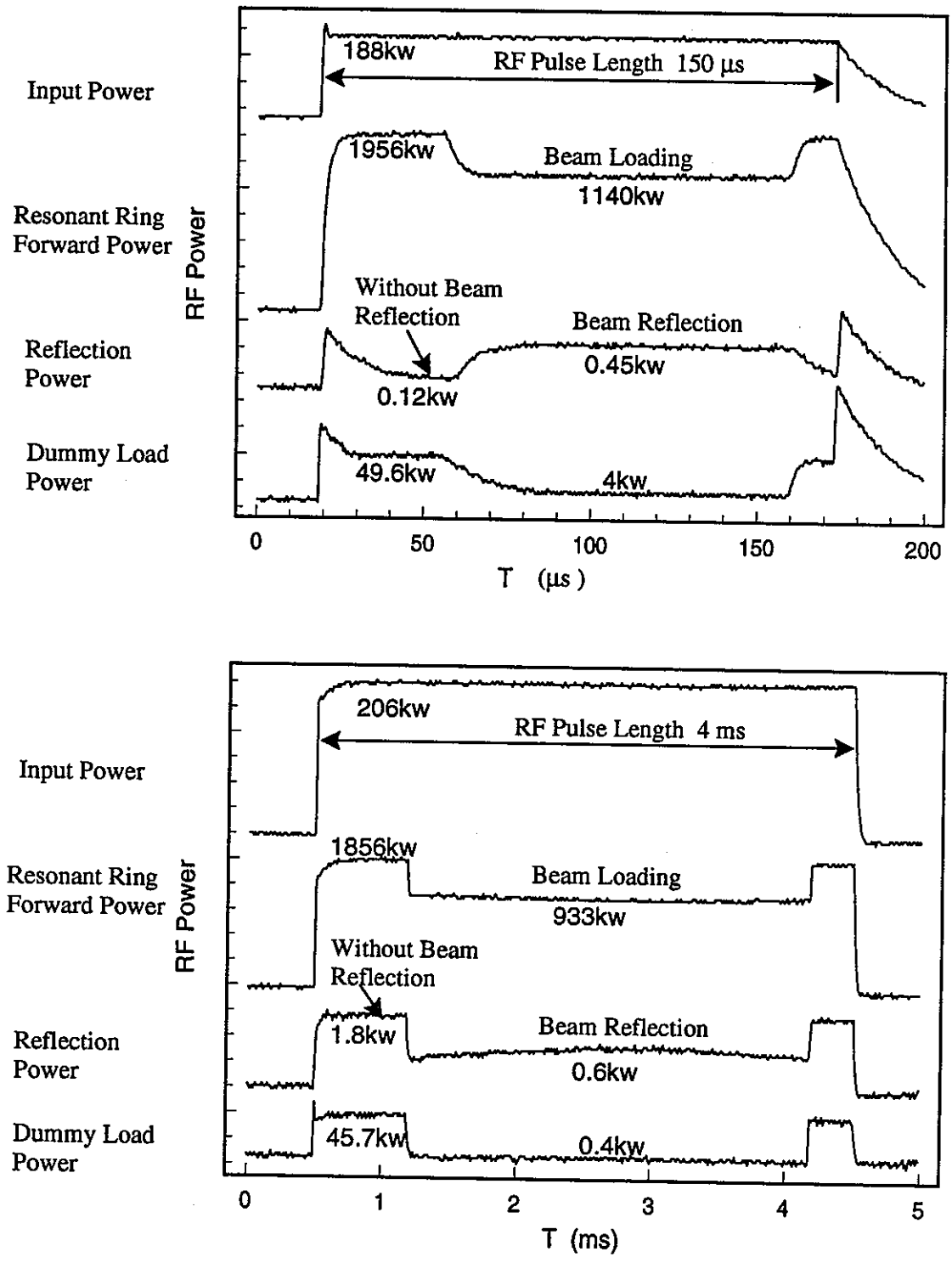

Fig. 13, Characteristics of RF in the TWRR for short and long pulses.

2), For the short pulse, without beam case, the reflection in the resonant ring is very small, with beam case, the beam reflection is a little bit large, the reflection coefficient Γ= 0.02; For the long pulse, without beam case, the reflection in the resonant ring is a little bit large(Γ=0.03), with beam case, the beam reflection becomes small, the reflection coefficient Γ= 0.025.

3), The power into the dummy load without beam case is large; with beam case becomes very small. It is an optimum for efficiency because we design the optimal coupling of TWRR at 100mA beam loading.

4-2, Phasing

For the phasing of the buncher and accelerator section, this time we used a way called resistive beam loading method. When the beam is in correct phase, a maximal energy is delivered to the beam, i.e. the RF power reduction is a maximum. When we adjusted the phase shifter in the waveguide system for each branch, according to the maximal beam loading in RF waveform to judge. It was not so sensitive, only rough adjustment. The energy spectrum is shown in Fig. 14.

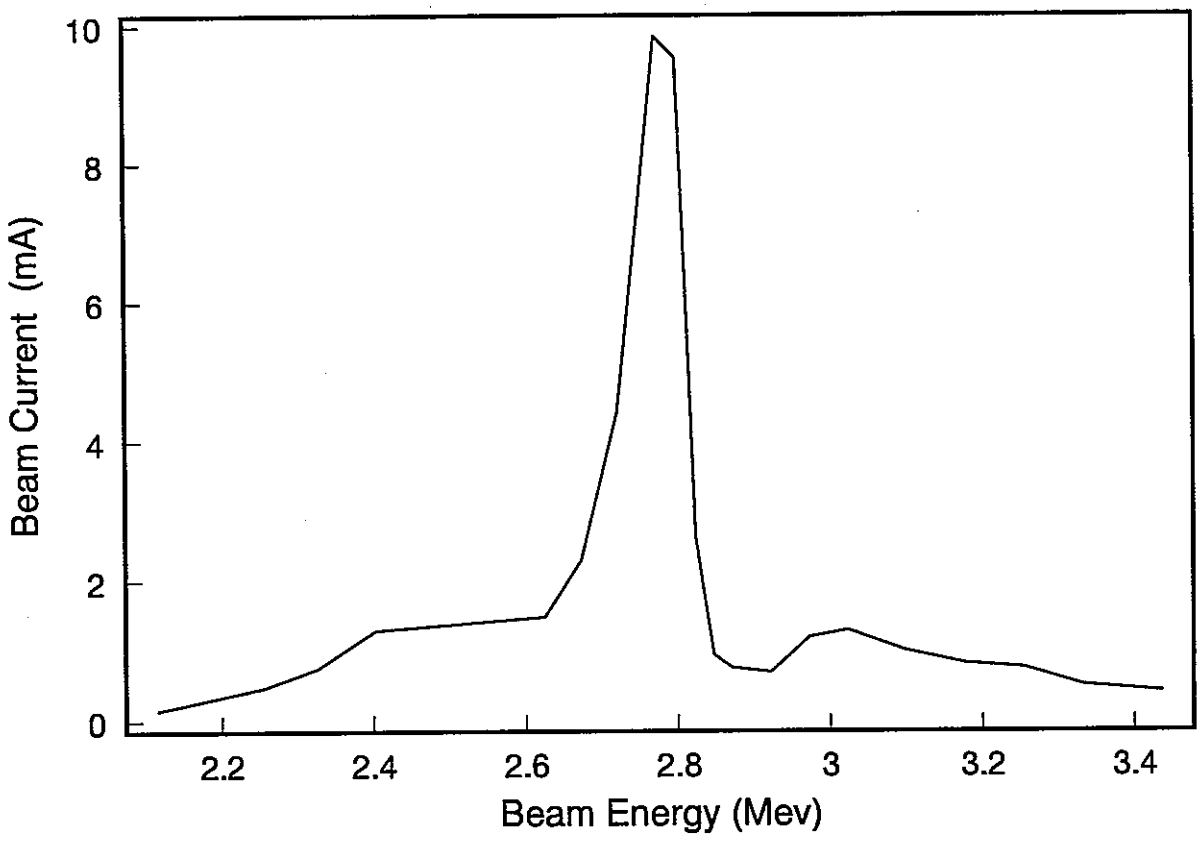

Fig. 14, Energy spectrum using the old slit (thickness 2mm, width 1mm)

4-3, Energy Spectra Measurement

From Fig.14 we can see that the energy spectrum has large background, it was caused by energy analyser slit too thin. Even though the slit was all close, some electrons still passed through the slit. Two kinds of structures of the energy analyser slits are shown in Fig.15. The lift side is old one which thickness is 2mm; the right side is new one which thickness is 10mm. After we changed the slit and Faraday cup the energy spectrum became only one peak and energy spread was about 1.4%. It is shown in Fig.16.

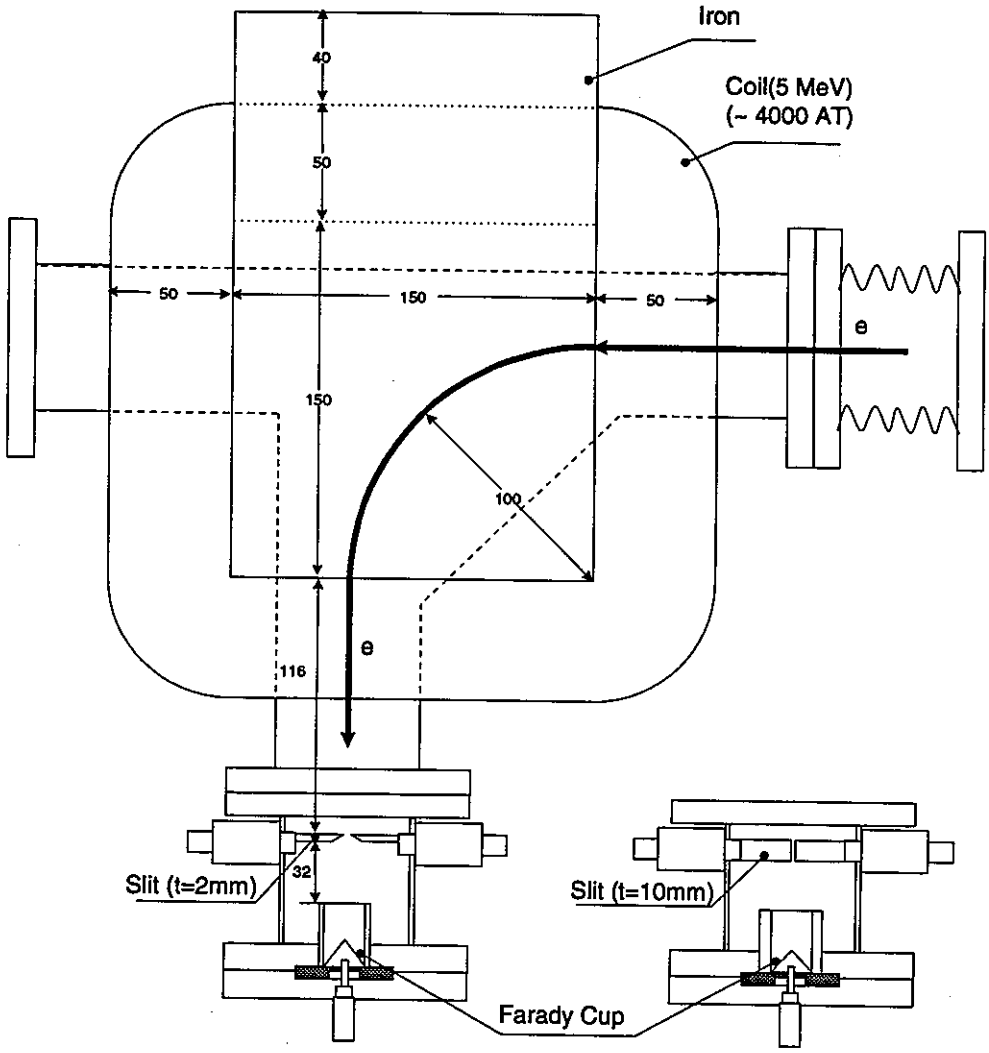

an old slit (thickness 2mm) a new slit (thickness 10mm)

Fig.15, Energy Analyser for 5Mev

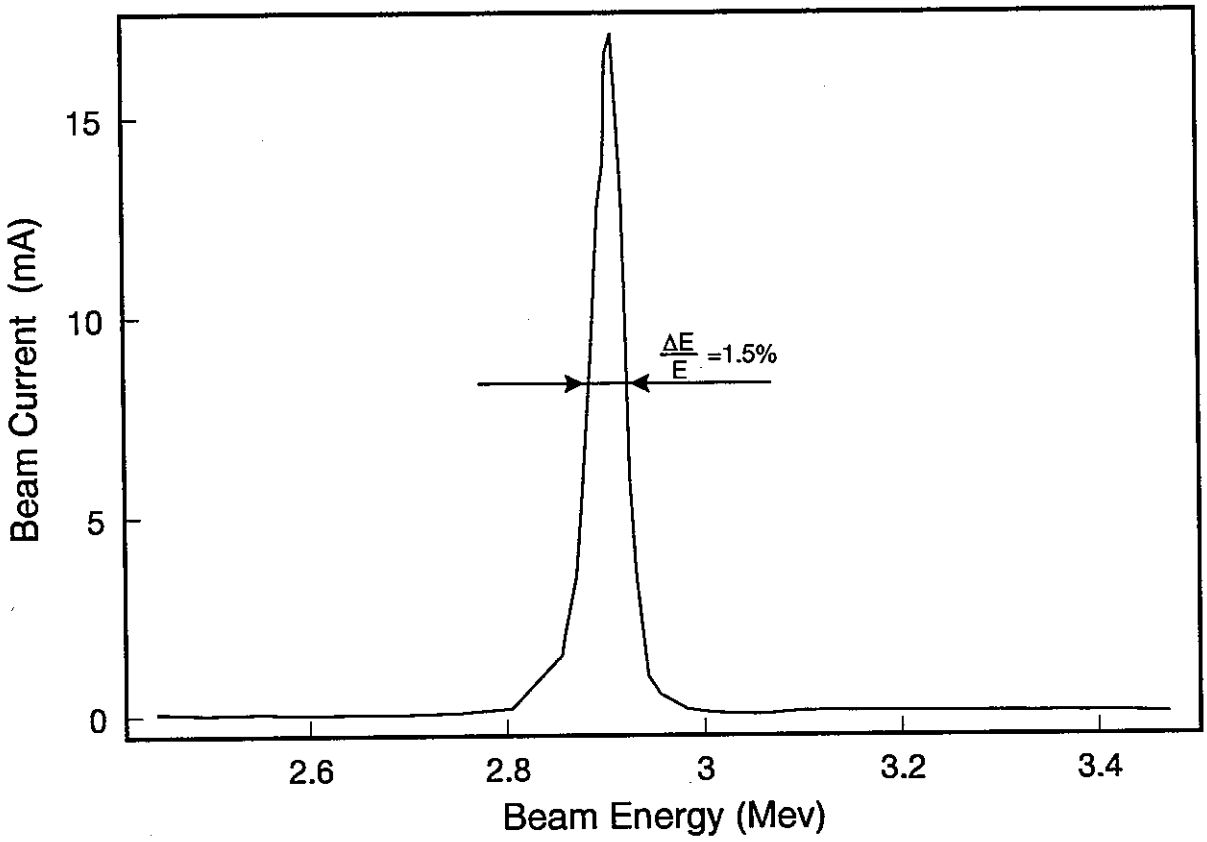

Fig. 16, Energy spectrum using the new slit (thickness 10mm, width 1mm)

4-4, Beam Loading Transient Effect

During the energy spectra measurement, the current from Faraday cup are shown in Fig.17. There are some high energy electrons in the beam pulse start and end parts. Because the filling time of TWRR with beam loading is about 5μs, for short pulse(~10μs) its effect is large, but for long pulse (~ms) it becomes very small. So only flat parts of beam pulses in Faraday cup were taken for our energy spectra measured data.

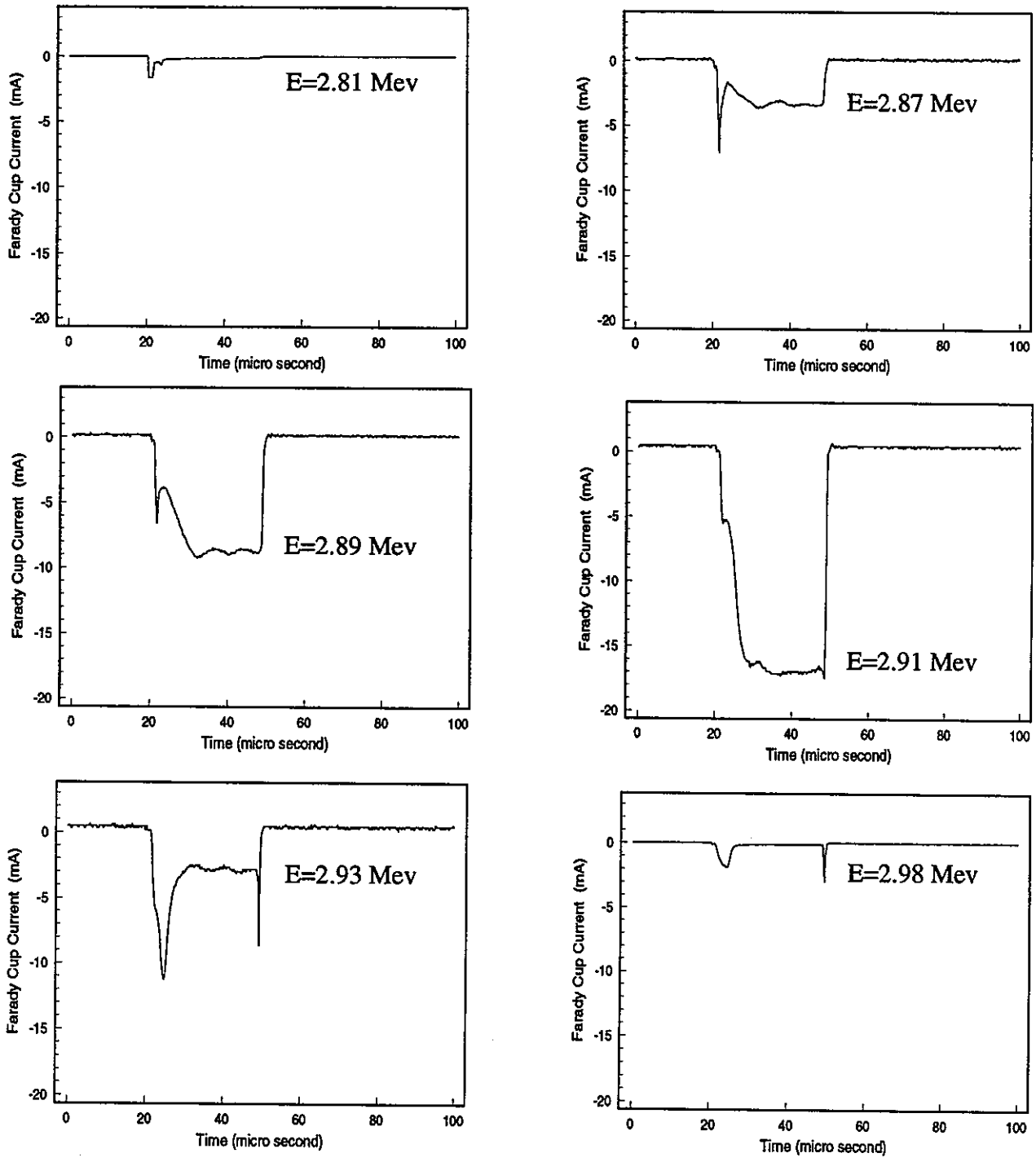

Fig.17, Current of Faraday cup during the energy spectra measurement

5, Summary

We were very smooth to finish the injector test in two months. The 100mA beam with pulse length 3ms and repetition rate 0.1Hz was accelerated to 3.0 MeV successfully. The beam energy spread was 1.5%. The measurement data are in good agreement with the design data. It shows important results that 1, using our design accelerator structure to accelerate 100mA beam with 3ms pulse is no problem, 2, the accelerator with TWRR has high efficiency, tuning and matching the TWRR is not so difficult, 3, the new chopper system will be very little emittance growth (the emittance has not been measured), making the chopper cavity resonance at two desirable modes is not so complicate, and 4, the injector is well to be adjusted and controlled.

Next, after all accelerator sections will be installed, we will do fine adjustments using the bunch length monitor , and use a reactive beam loading method to do phasing [6]. We will measure the beam emittance to check the action of our new type chopper system. We will accelerate 100mA beam to 10 MeV with 20% high duty (4ms, 50Hz). We will get a high quality beam, low emittance and small energy spread.

6, Acknowledgements

The authors wish to thank all members of our accelerator group for the test and discussions, to thank Prof. Sato and section leaders, who guided this test, to thank KEK linac group, who gave helpful discussions, and MHI members who help us to do the test.

7, References

[1] Y.L.Wang, et al. "Design of High Power Electron Linac at PNC", Journal of Nuclear Science and Technology,30[12],pp1261-1274, Dec. 1993

[2] Y.L.Wang, et al. "A Novel Chopper system for PNC High Power CW Linac", Proceedings of the 17th International Linac Conference, in Tsukuba Japan Aug. 1994, p205-207

[3], Y.L. Wang, et al. "A Novel Chopper System with Very little Emittance Growth." Proceedings of the 4th European Particle Accelerator Conference, in London, June 1994.

[4], Y.L. Wang, et al. "A New Chopper System with Low Emittance Growth. for PNC High Power CW Linac" Proceedings of the 19th Japan Linac Conference , in Tokai, July 1994

[5], Y.L.Wang, et al. "Chopper Cavity Test Report" Oct. 1994

[6], H.A.Hogg , et al. "The phasing system", The stanford two-mile accelerator p.385.